Journal of Medicinal Chemistry

Article

pubs.acs.org/jmc

Aldehyde Oxidase Mediated Metabolism in Drug-like Molecules: A Combined Computational and Experimental Study

Yuan Xu,[†,‡,#] Liang Li,[†,#] Yulan Wang,[†,‡,#] Jing Xing,[†,‡] Lei Zhou,[†,‡] Dafang Zhong,[†] Xiaomin Luo,[†] Hualiang Jiang,[†] Kaixian Chen,[†] Mingyue Zheng,[*,†] Pan Deng,[*,†] and Xiaoyan Chen[*,†]

[†]Shanghai Institute of Materia Medica, Chinese Academy of Sciences, Shanghai 201203, China

[‡]University of Chinese Academy of Sciences, No. 19A Yuquan Road, Beijing 100049, China

Supporting Information

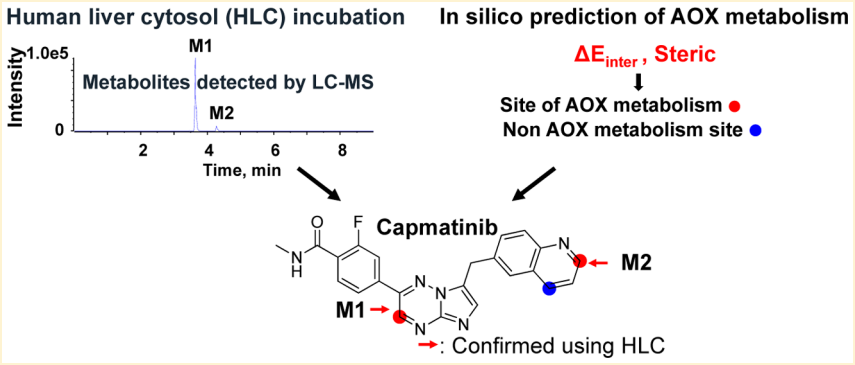

ABSTRACT: Aldehyde oxidase (AOX) is an important drug-metabolizing enzyme. However, the current in vitro models for evaluating AOX metabolism are sometimes misleading, and preclinical animal models generally fail to predict human AOX-mediated metabolism. In this study, we report a combined computational and experimental investigation of drug-like molecules that are potential aldehyde oxidase substrates, of which multiple sites of metabolism (SOMs) mediated by AOX and their preferences for the reaction can be unambiguously identified. In addition, the proposed strategy was used to evaluate the metabolism of newly designed c-Met inhibitors, and a success switch-off of AOX metabolism was observed. Overall, this study provide useful information to guide lead optimization and drug discovery based on AOX-mediated metabolism.

INTRODUCTION

Aldehyde oxidases (AOXs) are molybdenum-containing enzymes mainly located in the cytosolic compartment of cells.[1] They can metabolize various different functionalities, but the most important for drug development is the oxidation of aromatic azaheterocycles, including pyridines, benzimidazoles, diazines, purines, and a wide variety of other fused heteroaromatic systems.[2] The significance of AOXs as drug-metabolizing enzymes has been increasing because drug design is striving to reduce or remove cytochrome P450 metabolic liability, and because azaheterocycles, which can improve both pharmacokinetic and pharmacodynamic properties, have become popular building blocks in the synthesis of drug candidates. These chemical strategies, while generally successful, tend to produce chemical structures that are vulnerable to AOX metabolism.[3,4] According to Pryde et al.,[5] the proportion of potential AOX substrates among compounds that have already progressed to market is 13%, whereas the proportion is 45% for compounds under development at Pfizer. In addition, metabolic inactivation and toxicity resulted from AOX-catalyzed biotransformation were responsible for a series of drug failures in clinical trials,[6−9] for example **1** (RO1),[6] **2** (FK3453),[7] **3** (SGX523),[8] and **4** (JNJ-38877605)[9] (Figure 1), and this is predominantly caused by the current difficulties in predicting AOX-mediated metabolism during the preclinical phase of drug development.

AOX has several features that make it challenging to study AOX-catalyzed metabolism in preclinical settings. First, standard metabolic stability studies using liver microsomes always underestimate or overlook AOX-mediated metabolism because AOXs are mainly present in the cytosolic fraction. Second, the variability of AOX activities between different cytosol or S9 fraction preparations have been reported, and storage conditions may also affect AOX activity.[10−13] Moreover, in vivo studies on AOX-mediated metabolism in animal models are problematic because of the profound species differences.[10,14,15] The best proxies for human AOX metabolism are guinea pig and Rhesus monkey in terms of liver AOX expression.[16] However, these two models are not optimal because the expression of AOX isoenzymes in organs other than the liver may contribute to the overall metabolism of a compound. In this context, in silico methodologies could be used to predict whether a new molecule is a potential AOX

Received: January 6, 2017
Published: March 6, 2017

DOI: 10.1021/acs.jmedchem.7b00019
J. Med. Chem. 2017, 60, 2973−2982

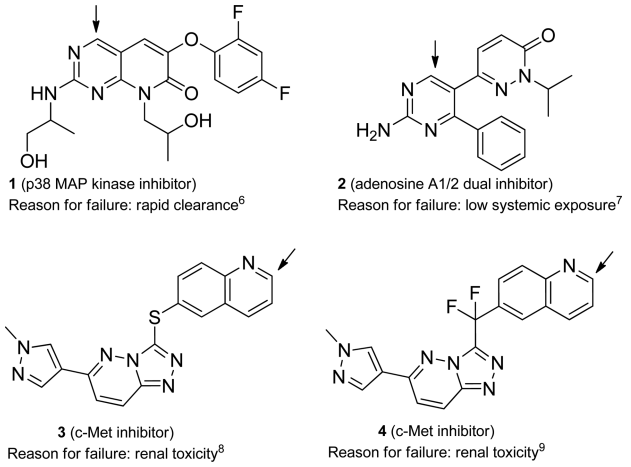

Figure 1. Examples of drug candidates that have been discontinued due to undesirable pharmacokinetic properties in humans or that have demonstrated toxicity attributed to AOX metabolism. Arrows indicate AOX metabolism sites.

substrate and may fill the gap left by the absence of reliable in vitro and in vivo metabolism models and the urgent need to evaluate AOX-catalyzed biotransformation in drug discovery. This could be of great importance to rational drug design and identification of AOX-related pharmacokinetics and safety problems early in drug development.

In contrast to the metabolism catalyzed by cytochrome P450, there are few in silico methods for predicting AOX metabolism. Torres et al. developed a model that used the heat of reaction of tetrahedral intermediate formation to predict the region selectivity of AOX metabolism.[17] The same strategy was adopted by Dalvie et al. to predict the differences in AOX metabolism rates for zoniporide analogues.[18] Recently, Jones et al. used the energy of the tetrahedral intermediate (ΔE_{inter}) and steric hindrance (**Steric**) as two descriptors to develop an intrinsic clearance prediction model for eight drugs metabolized by AOX.[19] In our preliminary experiment, this model was used in differentiating AOX substrate and nonsubstrate among 15 drug-like molecules using the criterion that "a low predicted clearance from this model would be a nonsubstrate". It was found that some intrinsic clearance predictions did not match with the experimental metabolism study, and there were some exceptions to this criterion. In addition, predicting the sites of metabolism (SOMs) is the key to developing new chemical entities, where screening potential metabolites for toxicity or unwanted side effects is particularly important. Therefore, the present study focused on the identification of SOMs for AOX using both computational and experimental approaches. First, a decision tree model was developed based on the two descriptors proposed by Jones et al.[19] Then, this model was applied to predicting SOMs in proprietary c-Met inhibitors and newly designed compounds intended to avoid AOX metabolism. In the end, the prediction results were verified using human liver cytosol incubation studies.

RESULTS

Construction of the Decision Tree Model for Predicting SOMs by AOX. As proposed by Jones et al., the AOX mediated metabolic clearance can be well characterized by two simple parameters: one is an electronic feature (ΔE_{inter}) that represents the energy changes between AOX substrate and its reaction intermediate, and the other is a steric feature (**Steric**) that represents the steric constraints associated with AOX and a predefined molecular probe.[19] In the present study, these two parameters were used to establish a decision tree model to predict potential SOMs in drug-like molecules for AOX. On the basis of 36 metabolic and 54 nonmetabolic sites collected from 35 compounds with known metabolic profiles, the decision tree was trained by using a SimpleCart algorithm.[20,21] Details about the calculation of parameters ΔE_{inter} and **Steric**, the computational modeling and validation results are provided in Supporting Information. The obtained decision tree for predicting the SOM of AOX (DT_{AOX}) is illustrated in Figure 2. At the first root note, a query site with a

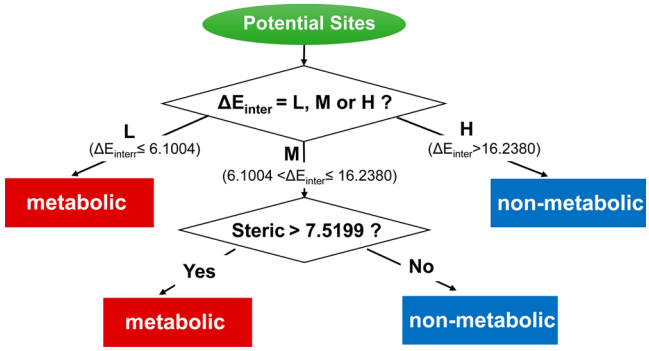

Figure 2. Decision tree model for the prediction of SOM catalyzed by AOX.

low ΔE_{inter} value was predicted as a SOM of AOX, whereas a site with a high ΔE_{inter} value was predicted as a nonmetabolic site. A lower ΔE_{inter} suggests that the intermediate is more stable and the site is more likely to be metabolized, whereas a higher ΔE_{inter} value represents an intermediate with a higher energy, which may lead to an unstable reaction. Sites with medium values of ΔE_{inter} were further divided by **Steric**, and sites with a **Steric** value greater than the threshold were predicted as a SOMs. Thus, when ΔE_{inter} falls into the medium range, it is the steric effect that has the greatest effect rather than the energy or the stability of intermediates. **Steric** describes the systematic energy reduction when the distance between the substrate and the probe is increased from 2.8 to 3.2 Å. This parameter was defined based on screening the distance between 2.2 and 7.0 Å that the most variant energy indicator between metabolic and nonmetabolic sites was chosen, which is different from the original definition. A larger **Steric** value suggests that the substrate is more sensitive to the spatial environment of the AOX active site captured by the designed probe. Therefore, using the parameters ΔE_{inter} and **Steric**, the decision tree clearly defined the rule for identifying site of AOX-mediated metabolism.

Prediction of the Single SOM Using the DT_{AOX} Model. Previous model used the lowest energy of the tetrahedral intermediate to predict the SOM of AOX, but energy alone would not always work well. Taking 2-aminopurine as an example (Figure 3a), the ΔE_{inter} value for site 1 fell into the medium range, which was not sufficient to determine the metabolism of this site. By including **Steric**, site 1 could be explicitly predicted as a nonmetabolic site. Additionally, for compound **5**, site 1 would be mistakenly predicted as a SOM if energy was the only criterion for metabolic site prediction (Figure 3b). After taking in account of **Steric**, this site was

DOI: 10.1021/acs.jmedchem.7b00019
J. Med. Chem. 2017, 60, 2973−2982

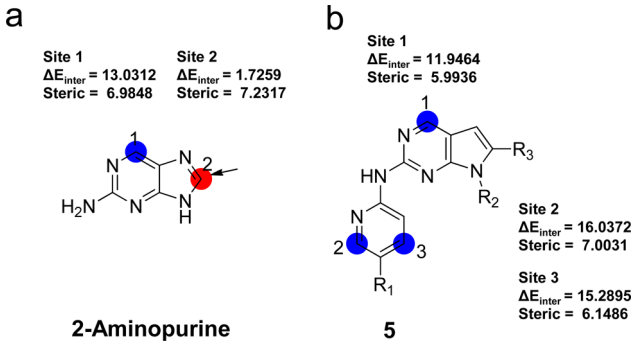

Figure 3. Prediction of SOM for 2-aminopurine (a) and **5** (b) using the DT_{AOX} model. The red and blue circles indicate the predicted metabolic and nonmetabolic sites, respectively. The experimentally observed SOM is marked with an arrow.

predicted as a nonmetabolic site, which was consistent with the experimental results.

Prediction of Multiple SOMs in AOX Substrates Using the DT_{AOX} Model. There are some known AOX substrates containing more than one site that can be metabolized, which presents a particular challenge to the existing computational models. Nevertheless, DT_{AOX} could evaluate all potential sites and identify multiple SOMs if exist. In the present study, four substrates with multiple SOMs were analyzed using the DT_{AOX} model (Table 1). For brimonidine, **6** (PF-04217903),[19] and quinazoline, the DT_{AOX} model clearly separated the SOMs from the other nonmetabolic sites. For pteridine, four sites were predicted as SOMs, whereas the experimentally observed AOX-catalyzed metabolites are produced from oxidation of sites 1 and 2. Site 3 has been reported as a SOM of xanthine oxidase,[17] which is another MoCo-containing enzyme. Overall, the DT_{AOX} model could efficiently identified multiple SOMs in

Table 1. Prediction of Multiple SOMs in AOX Substrates Using the DT_{AOX} Model[a]

Compounds	Site	Δ E_{inter} (kcal/mol)	Δ E_{inter} category	Steric (kJ/mol)	Predicted result	Experimental result
Brimonidine	1	8.7267	M	7.7478	Y	Y
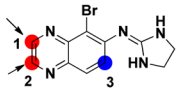	2	12.0592	M	7.8306	Y	Y
	3	24.5544	H	10.5358	N	N
6	1	10.5729	M	7.6026	Y	Y
	2	10.6338	M	8.1952	Y	Y
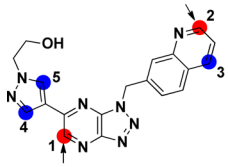	3	11.2806	M	3.6535	N	N
	4	23.8072	H	1.5229	N	N
	5	26.6788	H	3.6535	N	N
Pteridine	1	−0.9895	L	7.0269	Y	Y
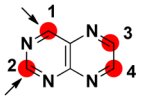	2	0.2288	L	7.2160	Y	Y
	3	8.3848	M	7.7117	Y	N
	4	−0.2859	L	7.5472	Y	N
Quinazoline	1	−6.8319	L	6.5005	Y	Y
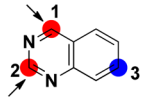	2	−5.1898	L	7.3036	Y	Y
	3	17.0759	H	7.2601	N	N

[a]The red and blue circles indicate the predicted metabolic and nonmetabolic sites, respectively. Experimentally observed SOMs are marked with arrows. L: low; M: medium; H: high; Y: SOM; N: nonmetabolic site.

DOI: 10.1021/acs.jmedchem.7b00019
J. Med. Chem. 2017, 60, 2973−2982

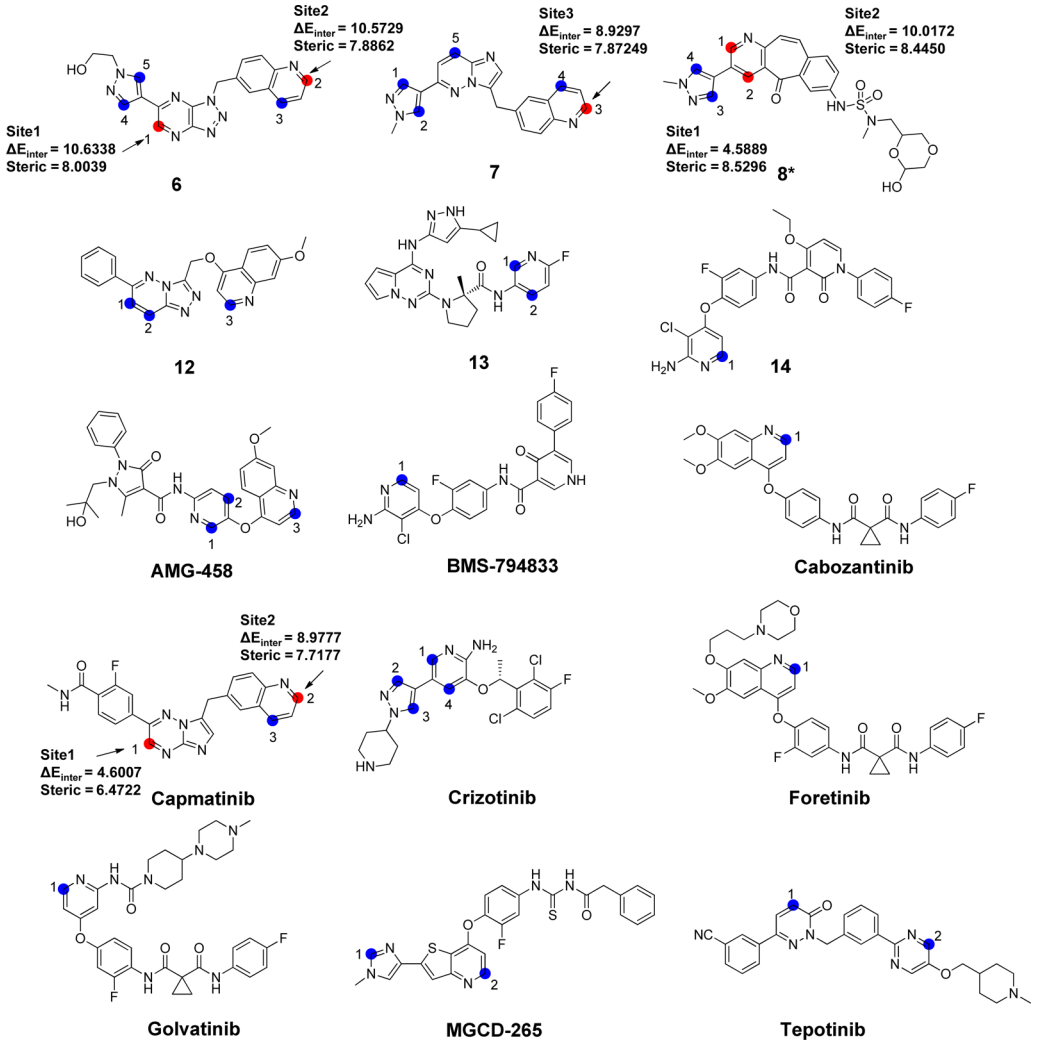

Figure 4. Predicted and observed AOX catalyzed SOMs for 15 c-Met inhibitors using the DT_{AOX}. Red and blue circles indicate the metabolic and nonmetabolic sites, respectively, predicted by DT_{AOX}. Experimental observed SOMs are marked with arrows. The values of two features for the predicted SOMs are listed. The asterisk (*) indicates the substrate with the false positive prediction.

a substrate, providing more comprehensive information about AOX catalyzed metabolism.

Screen AOX Substrates in c-Met Inhibitors Using the DT_{AOX} Model. Twenty-one c-Met inhibitors were obtained from Selleck (http://www.selleck.cn/pathways_c-Met.html), of which 15 compounds containing azaheterocycles could be potential substrates for AOX. Except for **6**,[19] the metabolism pathways of the other compounds have not been reported. All potential AOX metabolism sites of these c-Met inhibitors were labeled by matching predefined rules, and the DT_{AOX} model was used to predict the AOX metabolism. To validate the in silico prediction results, these compounds were incubated with human liver cytosol separately, and the samples were analyzed by ultraperformance liquid chromatography (UPLC)/quadrupole time-of-flight mass spectrometry (Q-TOF MS). Chemical inhibition studies were conducted to confirm the contribution of AOX to the metabolism of a given compound, in which a substantial decrease in the liquid chromatography−mass spectrometry (LC-MS) peak for an oxidative metabolite indicated the involvement of AOX and a substrate for AOX was therefore confirmed. On the basis of the DT_{AOX} model, one position in **7** (NVP-BVU972),[22] and two positions in **8** (MK-2461),[23] capmatinib, and **6** were predicted as SOMs (Figure 4), and the other 11 compounds were predicted as nonsubstrates for AOX. In human liver cytosol incubations, oxidative metabolites were detected in the samples containing **6**, **7**, and capmatinib as substrates (Figure 5). The chemical structures of the metabolites were proposed based on the fragment ion mass spectra (Figure 6). Co-incubation with AOX inhibitors hydralazine or menadione decreased the formation of these oxidative metabolites considerably (Table 2) and therefore confirmed the involvement of AOX in the metabolism of these four compounds. More details about the prediction and experimental results of all 15 c-Met inhibitors are given in Supporting Information, Table S3.

Evaluation of Chemical Approaches To Avoid AOX Metabolism. Examples of medicinal chemistry approaches that have successfully moved away from AOX-mediated oxidation in drug discovery have been described.[24] Those approaches included removing vulnerable SOMs and increasing steric bulk and electron density at the vulnerable heterocyclic ring. In silico prediction could evaluate the susceptibility of a compound to AOX metabolism quickly, guide structural optimization, and inform decisions about early biological AOX testing. In the present study, the AOX metabolism of three new c-Met inhibitors with azaheterocyclic skeletons

DOI: 10.1021/acs.jmedchem.7b00019
J. Med. Chem. 2017, 60, 2973−2982

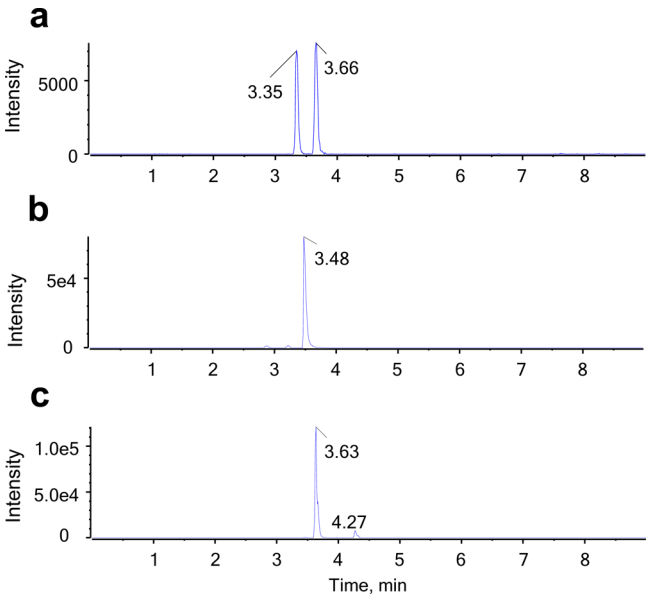

Figure 5. Extracted ion chromatographs of oxidative metabolites. (a) Compound **6** metabolites (m/z 389), (b) compound **7** metabolite (m/z 357), and (c) capmatinib metabolites (m/z 429) formed in human liver cytosol.

(Figure 7) were predicted using the established model, and the results were compared with the susceptibility to AOX of well-documented c-Met inhibitors **3**, **4**, and **6**. Compounds **9**, **10**, and **11** were designed using chemical approaches to prevent AOX metabolism. ΔE_{inter} and **Steric** of the six molecules are presented in Figure 7. In almost every instance, ΔE_{inter} fell into the medium range of the decision tree model; therefore, it is the steric effect that influences the AOX metabolism most rather than the energy or the stability of the intermediates. The **Steric** values for site 2 in compounds **9** and **10** were lower than 7.5199, and they fell into the category of nonsubstrates. Human cytosol incubation experiments indicated that the quinolone group could be metabolized in **3**, **4**, and **6** but not in compounds **9** and **10**. These results suggested that the R1 and R2 substitutions in compounds **9** and **10** changed the steric accessibility of the C-2 in quinolone and consequently decreased the AOX reactivity of this site. When the likely products of AOX metabolism for compound **11** were considered, a large difference in ΔE_{inter} values was observed, with ΔE_{inter} for site 1 being 10 times lower than for site 2 (Figure 7). Because the AOX metabolism rates are related to the stability of the tetrahedral intermediate formed during the reaction, the much lower ΔE_{inter} for site 1 suggested that the resulting tetrahedral intermediate was much more stable than that for site 2. This partially explained the observed metabolic profile of compound **11** in human liver cytosol (Supporting Information, Figure S4). The oxidation product at site 1 was identified as the major metabolite of compound **11**, and the metabolic turnover rate was high, with 50% of the substrate being oxidized after 30 min incubation in human liver cytosol. Therefore, for a compound with more than one SOM for AOX, ΔE_{inter} could be used to predict regioselectivity, and the lower ΔE_{inter}, the more favored the reaction.

DISCUSSION AND CONCLUSIONS

The AOX-catalyzed oxidation of *N*-heterocycles involves an initial nucleophilic attack at the carbon atom adjacent to the heteroatom, producing a tetrahedral intermediate.[25] The heat of reaction of the tetrahedral intermediate is used by some methods to predict the resulting oxidation product because of this proposed reaction mechanism. AOX substrates usually have more than one N atom, therefore multiple plausible oxidation sites may exist. It was reported that AOX substrates **6** and brimonidine have two AOX-catalyzed oxidative sites,[19,26,27] and the yields of two oxidative metabolites for each compound in vivo are comparable. For this type of substrate, it is important to identify all potential metabolic sites explicitly. The existing in silico prediction models are based solely on the energy of the tetrahedral intermediate, and they only predict the most likely SOM.[17,18] Using the present DT_{AOX} model, it was found that including steric features helped to identify multiple SOMs, e.g., **6** and brimonidine, and avoid false-positive predictions in **5**, which could be the case if only energy of the tetrahedral intermediate was used in predicting SOMs catalyzed by AOX.

In recent years, kinases have been identified as drug targets for a number of diseases, and the pharmacophores for these enzymes almost always include N atoms.[28] Among the known c-Met inhibitors, bicyclic triazole-based or triazine-based inhibitors have demonstrated high c-Met inhibitory potency and excellent selectivity against other kinases.[29] However, the development of many of these c-Met inhibitors has been terminated at the clinical trial or discovery stages because of toxicity or unexpectedly rapid metabolic clearance.[8,9] In the present study, the DT_{AOX} model was used to screen AOX substrates and identify SOMs in c-Met inhibitors. It was found that for campatinib, ΔE_{inter} of site 1 was much lower than site 2 according to the computational model predictions (Figure 4). UPLC/Q-TOF MS analysis showed that mono-oxidization on the imidazo[1,2-*b*][1,2,4]triazine (site 1 metabolism) produced the major metabolite of capmatinib in human liver cytosol (Figure 5c), and the LC-MS peak area was 10 times higher than that for the quinolone oxidative product (site 2 metabolism). These results suggested that the lower energy tetrahedral intermediate corresponded to the major oxidative metabolite. Therefore, when multiple SOMs exist in one compound, the site with the lowest ΔE_{inter} was preferentially metabolized. For **6**, the experimentally observed metabolites resulted from the oxidation of sites 1 and 2, and the amounts of these two oxidative metabolites were comparable based on the LC-MS peak areas (Figure 5a). This agreed with the similar ΔE_{inter} values for these two SOMs (Figure 4). Therefore, SOMs with similar energy changes in one compound could indicate a comparable degree of oxidation by AOX. Although two sites in **8** were predicted as SOMs by DT_{AOX} (site 1: ΔE_{inter} = 4.5889, **Steric** = 8.5296; site 2: ΔE_{inter} = 10.0172, **Steric** = 8.4450), no oxidized metabolite was detected in the corresponding human liver cytosol samples. One possible explanation for this false-positive prediction is the inaccurate tetrahedral intermediate structure, which was estimated by a geometry-optimized structure. Except for **8**, 15 c-Met inhibitors were correctly classified into substrates or nonsubstrates, showing a predicting accuracy of 93.33%.

Jones et. al have developed the first in silico models to predict both in vitro and in vivo human intrinsic clearance for AOX substrates using ΔE_{inter} and **Steric** as chemical descriptors.[19] In the present study, the application of this model in the prediction of AOX substrate was evaluated. The intrinsic clearance values of 15 compounds in Figure 4 were calculated using the linear equation (eq 2) described by Jones et. al.[19] It was found that the intrinsic clearance values of site 1

DOI: 10.1021/acs.jmedchem.7b00019
J. Med. Chem. 2017, 60, 2973−2982

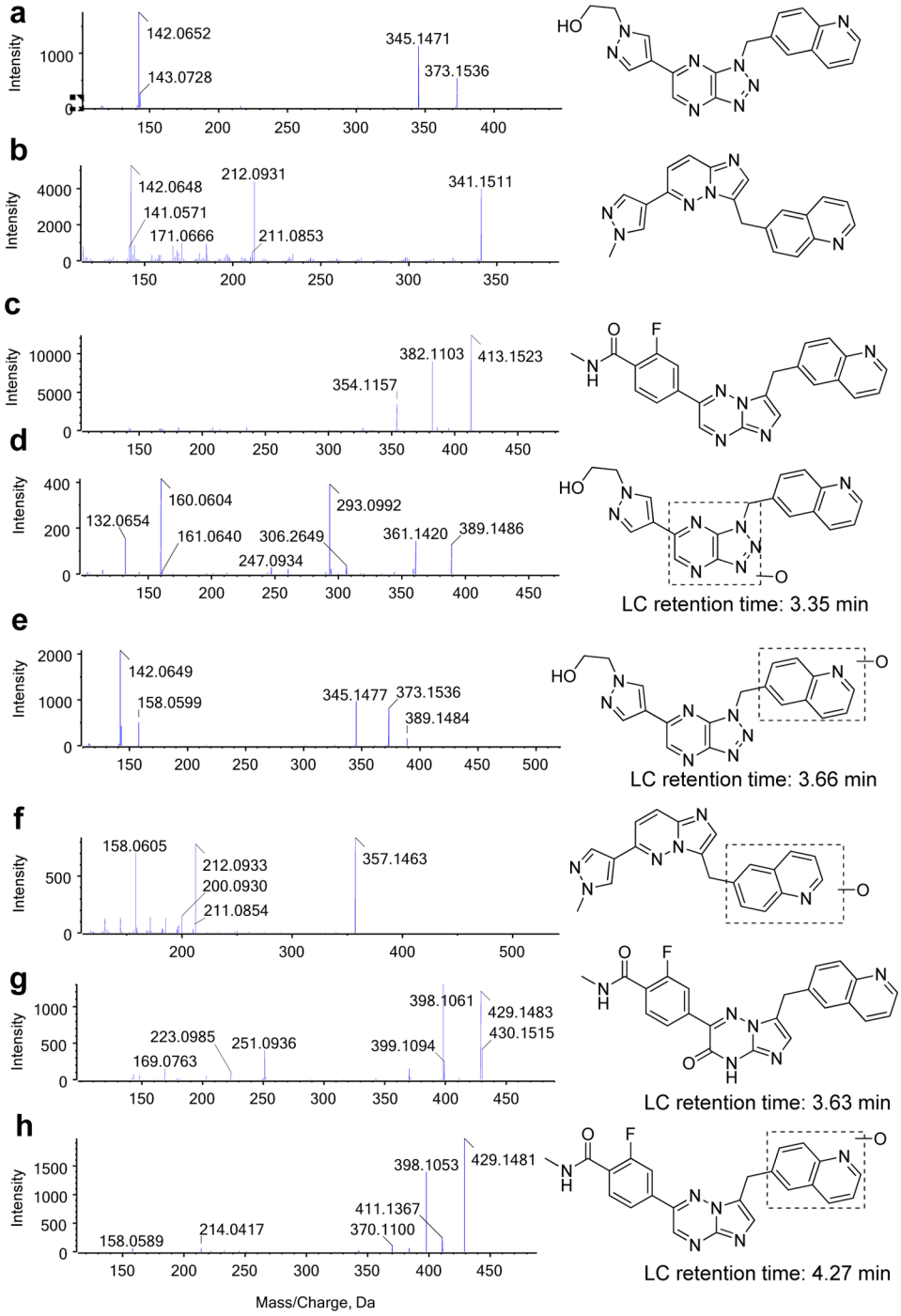

Figure 6. Product ion spectra of **6** (a), **7** (b), capmatinib (c), and their oxidative metabolites (d, e, f, g, and h) formed in human liver cytosol.

and site 2 in capmatinib were predicted as 2.60 and 1.70 mL/min/kg, respectively, and the value was 1.71 mL/min/kg for site 3 of **7**. Both of these two compounds are AOX substrates experimentally confirmed in our study. In contrast, the predicted intrinsic clearance values of the site 3 in **12** (AMG 208)[30] and the site 2 in tepotinib were higher than 1.71 mL/min/kg, but these two compounds are both nonsubstrates for AOX. In addition, the intrinsic clearance values of compounds **9** and **10** were predicted to be 1.89 and 1.63 mL/min/kg, respectively, however these two compounds are also nonsubstrates for AOX. Therefore, accurate prediction of AOX substrate can not be achieved by calculating intrinsic clearance using the in silico models proposed by Jones et al. For these cases, DT_{AOX} could more precisely distinguish nonmetabolic sites and multiple SOMs and decide whether a molecule is an AOX substrate. Overall, these results indicated that the current model could be used to identify AOX substrates and estimate the preference for oxidation when there are multiple SOMs.

Investigation of drug clearance catalyzed by AOX is important to drug development. In the present study, the same approach has been applied to build decision tree model for clearance prediction. On the basis of the available AOX mediated in vivo clearance data for 13 compounds, a new decision tree model was constructed, which only contained one splitting rule using **Steric**, while ΔE_{inter} was removed during tree-pruning. The overall prediction accuracy for the whole data

DOI: 10.1021/acs.jmedchem.7b00019
J. Med. Chem. 2017, 60, 2973−2982

Table 2. LC-MS Peak Areas of Oxidative Metabolites for 6, 7, and Capmatinib Incubated in Human Liver Cytosol Fractions with or without AOX Chemical Inhibitors[a]

		menadione		hydralazine	
metabolites	M_Area_without the inhibitor	M_Area_with the inhibitor	inhibition ratio (%)	M_Area_with the inhibitor	inhibition ratio (%)
6 site 1 oxidative metabolite	3.98×10^3	3.39×10^1	99.1	1.97×10^1	98.4
6 site 2 oxidative metabolite	1.22×10^4	1.98×10^2	99.5	ND	100
7 oxidative metabolites	1.80×10^5	9.10×10^3	94.9	ND	100
capmatinib site 1 oxidative metabolite	1.36×10^5	3.22×10^3	97.6	ND	100
capmatinib site 2 oxidative metabolite	2.03×10^4	8.45×10^2	95.8	ND	100

[a]M_Area: the LC-MS peak area of the metabolite; ND: not detected.

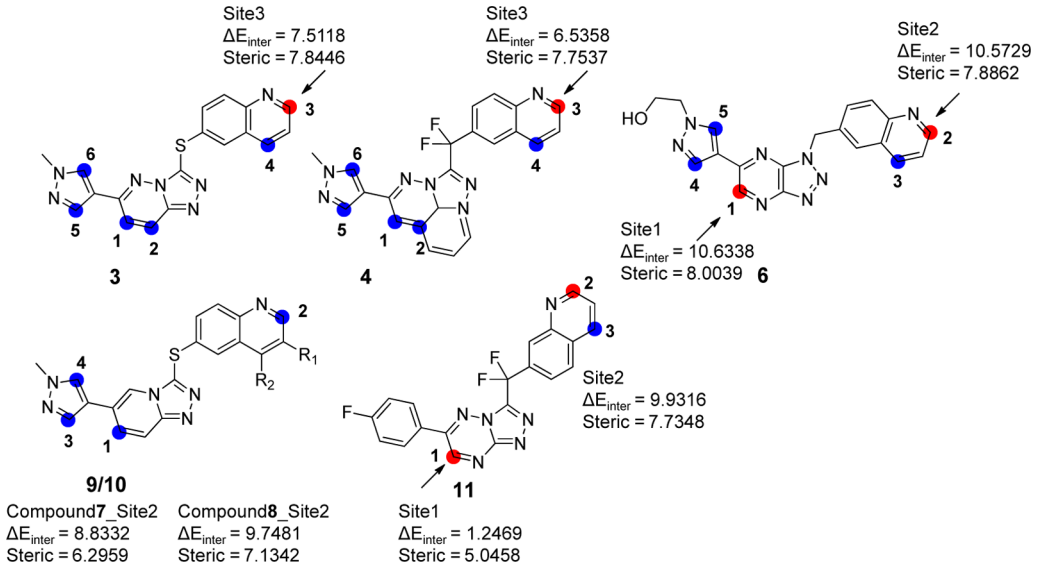

Figure 7. Predicted and observed AOX catalyzed SOM for six c-Met inhibitors with similar skeletons. The red and blue circles indicate the predicted metabolic and nonmetabolic sites, respectively. Two features ($\Delta E_{inter,}$ **Steric**) of these sites are listed. The arrows indicate the metabolic sites identified in human liver cytosols.

set was 0.7692. Further investigations are needed to establish a more accurate predictive model using abundant AOX mediated in vivo clearance data.

AOX is an important metabolic enzyme in drug development. In the present study, a DT_{AOX} model was developed to predict the SOMs of AOX. This model could identify multiple SOMs in a single compound and explained the metabolic regioselectivity. Additionally, this model was used to screen for AOX substrates in new c-Met kinase inhibitor drug candidates, and compounds with lower values of **Steric** avoided AOX metabolism. This study has increased our knowledge of AOX-mediated metabolism. Moreover, DT_{AOX} prediction may provide useful information for designing compounds with improved metabolic properties, which is of particular importance for the hit-to-lead optimization in drug development.

EXPERIMENTAL SECTION

Defining Potential SOMs and Tetrahedral Intermediate. On the basis of the catalytic mechanism and observed metabolites of AOX, two types of potential SOMs are defined (Table 3). In type A, the potential site is an aromatic ring carbon bearing one hydrogen and an aromatic nitrogen, and in the corresponding tetrahedral intermediates, a hydroxyl and a hydrogen are added to the oxidized carbon and the adjacent nitrogen, respectively. In type B, the potential site is a carbon bearing one hydrogen and involved in the conjugated addition with a γ-position nitrogen, and in the corresponding tetrahedral intermediates, a hydroxyl and a hydrogen are added to the oxidized carbon and the γ-position nitrogen, respectively. Type B includes transformations that occur less frequently, such as the metabolism reaction of *N*-[2-(dimethylamino)ethyl]acridine-4-carboxamide (DACA).[31]

Data Sets. The whole data set contains a total of 35 compounds. Of these, 31 compounds are known substrates of AOX collected from the literature[5,17] (Supporting Information, Table S4), and the other four are compounds synthesized in our lab (compound **5** in Figure 3, compounds **9**, **10**, and **11** in Figure 7). Altogether, 90 potential SOMs were identified using the structural patterns of these compounds, of which 36 sites that have been experimentally confirmed were labeled as "metabolic", and the other 54 sites were labeled as "non-metabolic". Here, a nonmetabolic site is an atom environment that matches the substructure pattern for AOX reaction but has not been experimentally identified as a SOM by AOX, and a metabolic site is a site that has been confirmed experimentally. A training set was prepared by randomly selecting 19 compounds from the published AOX substrates, including 21 metabolic and 29 nonmetabolic sites. The other 16 compounds were used as a test set that contains 15 metabolic and 25 nonmetabolic sites.

Development of the Prediction Model. The data for the 90 sites were grouped into a training set and a test set at a ratio of 5:4. A decision-tree-based classification model was constructed with the SimpleCart in Weka 3.0[32] using the classic Classification and Regression Trees (CART) algorithm,[20] an algorithm for decision trees that allows numerical target variables (regression).[21] The CART algorithm is a nonparametric approach that can deal with both

DOI: 10.1021/acs.jmedchem.7b00019
J. Med. Chem. 2017, 60, 2973−2982

Table 3. Two Types of Potential SOMs by AOX[a]

Type	Descriptions	SMARTS*	Representative substrates/sites	Representative intermediates
A	Aromatic ring carbon bearing one hydrogen and an aromatic nitrogen	[cH]:n	**3** 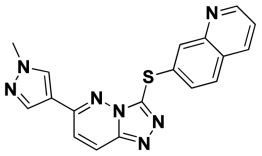	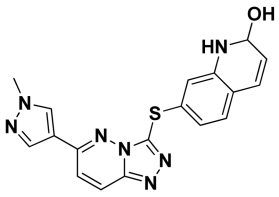
B	Carbon bearing one hydrogen and involved in the conjugated addition with γ-position nitrogen	[cH] = [*;R] ~ [*;R] = n	DACA 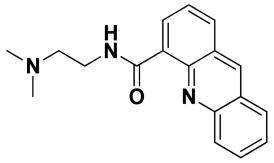	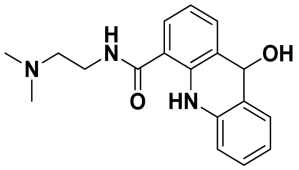

[a]*SMARTS: SMiles ARbitrary Target Specification.

categorical and numeric dependent variables. On the basis of the Gini Index (https://en.wikipedia.org/wiki/Gini_coefficient), which measures the impurity of nodes, the CART method produces a binary split so that the full data set is split into two smaller subsets at the root node. Then, each subset is split recursively until all data in the node is of the same class or the purity of the node cannot be increased. The decision tree model for predicting the SOM of AOX was constructed with ΔE_{inter} and **Steric** by using open resource software WEKA (http://www.cs.waikato.ac.nz/ml/weka/). numFoldsPruning, which is the number of folds in the internal CV, was set as 49 to conduct LOO CV. The minimum number of observations at the terminal nodes was set as 8 to avoid an overly complex tree. Other parameters in WEKA were set as their default values.

Human Liver Cytosol Incubations of c-Met Kinase Inhibitors. Pooled human liver cytosol (XenoTech, KS, USA) incubations were conducted in 100 mM potassium phosphate buffer (PBS, pH 7.4). Individual stock solution (10 mM) of c-Met kinase inhibitors was prepared in dimethyl sulfoxide (DMSO). The final concentration of DMSO in the incubation mixture was 0.1% (v/v). The reaction mixtures contained 0.5 mg/mL human liver cytosol protein. The final incubation volume was 200 μL. After 3 min of preincubation at 37 °C, the reactions were initiated with the addition of 10 μM substrate (final concentration). The reactions were terminated with an equal volume of ice-cold acetonitrile after 30 min of incubation. Control experiments were performed with no test compound or with inactivated enzymes. Each incubation was performed in duplicate.

UPLC/Q-TOF MS Analysis. Incubation samples were vortex-mixed and centrifuged at 14000*g* for 5 min. A 5 μL aliquot of the supernatant was injected for the UPLC/Q-TOF MS analysis. The chromatographic separation of c-Met kinase inhibitors and their metabolites was achieved using an UPLC system (Acquity, Waters, Milford, MA, USA) on an HSS T3 column (Acquity, Waters, 1.8 μm, 100 mm × 2.1 mm i.d.). The mobile phase was a mixture of 5 mM ammonium acetate containing 0.1% formic acid (A) and acetonitrile (B). Gradient elution started from 10% B maintained for 1 min, increased linearly to 65% B over 6 min, increased linearly to 99% B over 0.5 min, held at 99% B for another 1.5 min, and finally, reduced to 10% B to re-equilibrate the column. The column was set at 45 °C and the flow rate was 0.4 mL/min.

Q-TOF MS analysis was performed in positive ion mode (TripleTOF 5600+, Sciex, Concord, Ontario, Canada) using a DuoSpray ion source (Sciex). The instrument was automatically

DOI: 10.1021/acs.jmedchem.7b00019
J. Med. Chem. 2017, 60, 2973−2982

calibrated every five injections by using an external calibration system. The ion source conditions were set as follows: ion source gas 1 and gas 2, 55, and 50 (arbitrary units), respectively; temperature, 550 °C; curtain gas, 40 (arbitrary units); ion-spray voltage floating, 5.5 kV; and declustering potential, 70 V. Data were acquired via an information-dependent acquisition (IDA) method, which was performed using Analyst TF 1.6 (Sciex). The IDA method involved a TOF MS scan (collision energy, 10 eV) and three dependent product ion scans (collision energy, 45 ± 15 eV, 30 ± 15 eV, and 20 ± 10 eV) in high-sensitivity mode with dynamic background subtraction. The multiple mass defect filter (MDF window, ± 40 mDa; mass range, ± 50 Da) function was used. The TOF MS and product ion scans ranged from m/z 80 to 1000.

Enzyme Metabolism Inhibition Studies. The involvement of AOX in the oxidative metabolism of c-Met kinase inhibitors (crizotinib, tepotinib, capmatinib, golvatinib, **3**, **4**, **6**, **7**, **11**, **13** (BMS-754807),[33] and **14** (BMS-777607)[34]) were further investigated by incubating individual c-Met kinase inhibitors with two AOX chemical inhibitors (100 μM menadione or 100 μM hydralazine). The inhibitors were dissolved in DMSO, and the final concentration of DMSO in the incubation was 0.2% (v/v). The incubation mixtures contained 0.5 mg/mL human liver cytosol protein and the individual inhibitors in 100 mM PBS. The final incubation volume was 200 μL. After 10 min of preincubation at 37 °C, the reactions were initiated with the addition of 10 μM of substrate (final concentration). The reactions were terminated with an equal volume of ice-cold acetonitrile after 30 min of incubation. Controls without chemical inhibitors were included. Each incubation was performed in duplicate.

■ ASSOCIATED CONTENT

Supporting Information

The Supporting Information is available free of charge on the ACS Publications website at DOI: 10.1021/acs.jmedchem.7b00019.

Defining potential SOMs and tetrahedral intermediate; calculation of ΔE_{inter} and **Steric**; construction of the decision tree model; applicability domain; metabolic profiles of new c-Met inhibitors in human liver cytosol for compounds **9**−**11**; predicted and experimental results for AOX metabolism of 15 c-Met kinase inhibitors; structures of the 31 AOX substrates (PDF)

Molecular formula strings (CSV)

■ AUTHOR INFORMATION

Corresponding Authors

*For M.Y.Z.: phone, +86-21-50271399; e-mail, myzheng@simm.ac.cn.

*For P.D.: phone, +86-21-50800738; e-mail, panda4177@gmail.com.

*For X.Y.C.: phone, +86-21-50800738; e-mail, xychen@simm.ac.cn.

ORCID

Mingyue Zheng: 0000-0002-3323-3092

Pan Deng: 0000-0003-2974-7389

Xiaoyan Chen: 0000-0002-6559-8627

Author Contributions

The manuscript was written through contributions of all authors.

Author Contributions

#Y.X., L.L., and Y.W. contributed equally to this work.

Notes

The authors declare no competing financial interest.

■ ACKNOWLEDGMENTS

We gratefully acknowledge financial support from the National Natural Science Foundation of China (81573500), the Strategic Priority Research Program of the Chinese Academy of Sciences (XDA12050201), and the National Key Research & Development (R&D) Plan (2016YF1201003).

■ ABBREVIATIONS USED

AOX, aldehyde oxidase; CART, classification and regression trees; CV, cross validation; DT_1, decision tree only contains a single node; DMSO, dimethyl sulfoxide; DT_{AOX}, decision tree for predicting the site of metabolism of aldehyde oxidase; ΔE_{inter}, intermediate formation energy; IDA, information dependent acquisition; LC-MS, liquid chromatography−mass spectrometry; LOO, leave one out; MDF, mass defect filter; ND, not detected; Q-TOF MS, quadrupole time-of-flight mass spectrometry; SOM, site of metabolism; **Steric**, steric hindrance feature; UPLC, ultraperformance liquid chromatography

■ REFERENCES

(1) Garattini, E.; Fratelli, M.; Terao, M. The mammalian aldehyde oxidase gene family. *Hum. Genomics* **2009**, *4*, 119−130.

(2) Sanoh, S.; Tayama, Y.; Sugihara, K.; Kitamura, S.; Ohta, S. Significance of aldehyde oxidase during drug development: Effects on drug metabolism, pharmacokinetics, toxicity, and efficacy. *Drug Metab. Pharmacokinet.* **2015**, *30*, 52−63.

(3) Garattini, E.; Terao, M. Increasing recognition of the importance of aldehyde oxidase in drug development and discovery. *Drug Metab. Rev.* **2011**, *43*, 374−386.

(4) Garattini, E.; Terao, M. Aldehyde oxidase and its importance in novel drug discovery: present and future challenges. *Expert Opin. Drug Discovery* **2013**, *8*, 641−654.

(5) Pryde, D. C.; Dalvie, D.; Hu, Q.; Jones, P.; Obach, R. S.; Tran, T. D. Aldehyde oxidase: an enzyme of emerging importance in drug discovery. *J. Med. Chem.* **2010**, *53*, 8441−8460.

(6) Zhang, X.; Liu, H. H.; Weller, P.; Zheng, M.; Tao, W.; Wang, J.; Liao, G.; Monshouwer, M.; Peltz, G. In silico and in vitro pharmacogenetics: aldehyde oxidase rapidly metabolizes a p38 kinase inhibitor. *Pharmacogenomics J.* **2011**, *11*, 15−24.

(7) Akabane, T.; Tanaka, K.; Irie, M.; Terashita, S.; Teramura, T. Case report of extensive metabolism by aldehyde oxidase in humans: pharmacokinetics and metabolite profile of FK3453 in rats, dogs, and humans. *Xenobiotica* **2011**, *41*, 372−384.

(8) Infante, J. R.; Rugg, T.; Gordon, M.; Rooney, I.; Rosen, L.; Zeh, K.; Liu, R.; Burris, H. A.; Ramanathan, R. K. Unexpected renal toxicity associated with SGX523, a small molecule inhibitor of MET. *Invest. New Drugs* **2013**, *31*, 363−369.

(9) Lolkema, M.; Bohets, H. H.; Arkenau, H. T.; Lampo, A.; Barale, E.; de Jonge, M. J. A.; van Doorn, L.; Hellemans, P.; de Bono, J.; Eskens, F. A. The c-Met tyrosine kinase inhibitor JNJ-38877605 causes renal toxicity through species specific insoluble metabolite formation. *Clin. Cancer Res.* **2015**, *21*, 2297−2304.

(10) Sahi, J.; Khan, K. K.; Black, C. B. Aldehyde oxidase activity and inhibition in hepatocytes and cytosolic fractions from mouse, rat, monkey and human. *Drug Metab. Lett.* **2008**, *2*, 176−183.

(11) Duley, J. A.; Harris, O.; Holmes, R. S. Analysis of human alcohol- and aldehyde-metabolizing isozymes by electrophoresis and isoelectric focusing. *Alcohol.: Clin. Exp. Res.* **1985**, *9*, 263−271.

(12) Al-Salmy, H. S. Individual variation in hepatic aldehyde oxidase activity. *IUBMB Life* **2001**, *51*, 249−253.

(13) Zientek, M. A.; Youdim, K. Reaction phenotyping: advances in the experimental strategies used to characterize the contribution of drug-metabolizing enzymes. *Drug Metab. Dispos.* **2015**, *43*, 163−181.

(14) Dalvie, D.; Xiang, C.; Kang, P.; Zhou, S. Interspecies variation in the metabolism of zoniporide by aldehyde oxidase. *Xenobiotica* **2013**, *43*, 399−408.

DOI: 10.1021/acs.jmedchem.7b00019
J. Med. Chem. 2017, 60, 2973−2982

(15) Diamond, S.; Boer, J.; Maduskuie, T. P., Jr.; Falahatpisheh, N.; Li, Y.; Yeleswaram, S. Species-specific metabolism of SGX523 by aldehyde oxidase and the toxicological implications. *Drug Metab. Dispos.* **2010**, *38*, 1277−1285.
(16) Choughule, K. V.; Barr, J. T.; Jones, J. P. Evaluation of rhesus monkey and guinea pig hepatic cytosol fractions as models for human aldehyde oxidase. *Drug Metab. Dispos.* **2013**, *41*, 1852−1858.
(17) Torres, R. A.; Korzekwa, K. R.; McMasters, D. R.; Fandozzi, C. M.; Jones, J. P. Use of density functional calculations to predict the regioselectivity of drugs and molecules metabolized by aldehyde oxidase. *J. Med. Chem.* **2007**, *50*, 4642−4647.
(18) Dalvie, D.; Sun, H.; Xiang, C.; Hu, Q.; Jiang, Y.; Kang, P. Effect of structural variation on aldehyde oxidase-catalyzed oxidation of zoniporide. *Drug Metab. Dispos.* **2012**, *40*, 1575−1587.
(19) Jones, J. P.; Korzekwa, K. R. Predicting intrinsic clearance for drugs and drug candidates metabolized by aldehyde oxidase. *Mol. Pharmaceutics* **2013**, *10*, 1262−1268.
(20) Breiman, L.; Friedman, J.; Stone, C. J.; Olshen, R. A. *Classification and Regression Trees*; Chapman and Hall/CRC: Boca Raton, FL, 1984.
(21) Henrard, S.; Speybroeck, N.; Hermans, C. Classification and regression tree analysis vs. multivariable linear and logistic regression methods as statistical tools for studying haemophilia. *Haemophilia* **2015**, *21*, 715−722.
(22) Tiedt, R.; Degenkolbe, E.; Furet, P.; Appleton, B. A.; Wagner, S.; Schoepfer, J.; Buck, E.; Ruddy, D. A.; Monahan, J. E.; Jones, M. D.; Blank, J.; Haasen, D.; Drueckes, P.; Wartmann, M.; McCarthy, C.; Sellers, W. R.; Hofmann, F. A drug resistance screen using a selective MET inhibitor reveals a spectrum of mutations that partially overlap with activating mutations found in cancer patients. *Cancer Res.* **2011**, *71*, 5255−5264.
(23) Katz, J. D.; Jewell, J. P.; Guerin, D. J.; Lim, J.; Dinsmore, C. J.; Deshmukh, S. V.; Pan, B. S.; Marshall, C. G.; Lu, W.; Altman, M. D.; Dahlberg, W. K.; Davis, L.; Falcone, D.; Gabarda, A. E.; Hang, G.; Hatch, H.; Holmes, R.; Kunii, K.; Lumb, K. J.; Lutterbach, B.; Mathvink, R.; Nazef, N.; Patel, S. B.; Qu, X.; Reilly, J. F.; Rickert, K. W.; Rosenstein, C.; Soisson, S. M.; Spencer, K. B.; Szewczak, A. A.; Walker, D.; Wang, W.; Young, J.; Zeng, Q. Discovery of a 5H-benzo[4,5]cyclohepta[1,2-b]pyridin-5-one (MK-2461) inhibitor of c-Met kinase for the treatment of cancer. *J. Med. Chem.* **2011**, *54*, 4092−4108.
(24) Pryde, D. C.; Tran, T. D.; Jones, P.; Duckworth, J.; Howard, M.; Gardner, I.; Hyland, R.; Webster, R.; Wenham, T.; Bagal, S.; Omoto, K.; Schneider, R. P.; Lin, J. Medicinal chemistry approaches to avoid aldehyde oxidase metabolism. *Bioorg. Med. Chem. Lett.* **2012**, *22*, 2856−2860.
(25) Alfaro, J. F.; Jones, J. P. Studies on the mechanism of aldehyde oxidase and xanthine oxidase. *J. Org. Chem.* **2008**, *73*, 9469−9472.
(26) Ni, J.; Rowe, J.; Heidelbaugh, T.; Sinha, S.; Acheampong, A. Characterization of benzimidazole and other oxidative and conjugative metabolites of brimonidine in vitro and in rats in vivo using on-line HID exchange LC-MS/MS and stable-isotope tracer techniques. *Xenobiotica* **2007**, *37*, 205−220.
(27) Acheampong, A. A.; Chien, D. S.; Lam, S.; Vekich, S.; Breau, A.; Usansky, J.; Harcourt, D.; Munk, S. A.; Nguyen, H.; Garst, M.; Tang-Liu, D. Characterization of brimonidine metabolism with rat, rabbit, dog, monkey and human liver fractions and rabbit liver aldehyde oxidase. *Xenobiotica* **1996**, *26*, 1035−1055.
(28) Muller, S.; Chaikuad, A.; Gray, N. S.; Knapp, S. The ins and outs of selective kinase inhibitor development. *Nat. Chem. Biol.* **2015**, *11*, 818−821.
(29) Li, C.; Ai, J.; Zhang, D.; Peng, X.; Chen, X.; Gao, Z.; Su, Y.; Zhu, W.; Ji, Y.; Chen, X.; Geng, M.; Liu, H. Design, synthesis, and biological evaluation of novel imidazo[1,2-a]pyridine derivatives as potent c-Met inhibitors. *ACS Med. Chem. Lett.* **2015**, *6*, 507−512.
(30) Hong, D. S.; Rosen, P.; Lockhart, A. C.; Fu, S.; Janku, F.; Kurzrock, R.; Khan, R.; Amore, B.; Caudillo, I.; Deng, H.; Hwang, Y. C.; Loberg, R.; Ngarmchamnanrith, G.; Beaupre, D. M.; Lee, P. A first-in-human study of AMG 208, an oral MET inhibitor, in adult patients with advanced solid tumors. *Oncotarget* **2015**, *6*, 18693−18706.
(31) Barr, J. T.; Jones, J. P. Inhibition of human liver aldehyde oxidase: implications for potential drug-drug interactions. *Drug Metab. Dispos.* **2011**, *39*, 2381−2386.
(32) Hall, M.; Frank, E.; Holmes, G.; Pfahringer, B.; Reutemann, P.; Witten, I. H. The WEKA data mining software: an update. *SIGKDD Explor.* **2009**, *11*, 10−18.
(33) Wittman, M. D.; Carboni, J. M.; Yang, Z.; Lee, F. Y.; Antman, M.; Attar, R.; Balimane, P.; Chang, C.; Chen, C.; Discenza, L.; Frennesson, D.; Gottardis, M. M.; Greer, A.; Hurlburt, W.; Johnson, W.; Langley, D. R.; Li, A.; Li, J.; Liu, P.; Mastalerz, H.; Mathur, A.; Menard, K.; Patel, K.; Sack, J.; Sang, X.; Saulnier, M.; Smith, D.; Stefanski, K.; Trainor, G.; Velaparthi, U.; Zhang, G.; Zimmermann, K.; Vyas, D. M. Discovery of a 2,4-disubstituted pyrrolo[1,2-f][1,2,4]-triazine inhibitor (BMS-754807) of insulin-like growth factor receptor (IGF-1R) kinase in clinical development. *J. Med. Chem.* **2009**, *52*, 7360−7363.
(34) Schroeder, G. M.; An, Y.; Cai, Z. W.; Chen, X. T.; Clark, C.; Cornelius, L. A.; Dai, J.; Gullo-Brown, J.; Gupta, A.; Henley, B.; Hunt, J. T.; Jeyaseelan, R.; Kamath, A.; Kim, K.; Lippy, J.; Lombardo, L. J.; Manne, V.; Oppenheimer, S.; Sack, J. S.; Schmidt, R. J.; Shen, G.; Stefanski, K.; Tokarski, J. S.; Trainor, G. L.; Wautlet, B. S.; Wei, D.; Williams, D. K.; Zhang, Y.; Zhang, Y.; Fargnoli, J.; Borzilleri, R. M. Discovery of N-(4-(2-amino-3-chloropyridin-4-yloxy)-3-fluorophenyl)-4-ethoxy-1-(4-fluorophenyl)-2-oxo-1,2-dihydropyridine-3-carboxamide (BMS-777607), a selective and orally efficacious inhibitor of the Met kinase superfamily. *J. Med. Chem.* **2009**, *52*, 1251−1254.

DOI: 10.1021/acs.jmedchem.7b00019
J. Med. Chem. 2017, 60, 2973−2982